

High Selectivity Balanced Bandpass Filter with Tunable Bandwidth Using Stub-Loaded Resonator

Yalin Ma^{1, 2}, Wenquan Che¹, Jianxin Chen³, and Wenjie Feng^{1, *}

Abstract—A new balanced bandpass filter (BPF) with tunable bandwidth using tri-mode stub-loaded resonators is proposed. To tune the differential-mode bandwidth, the two even-mode resonance frequencies and two transmission zeros (TZs) are tuned while the odd-mode resonance frequency keeps unchanged. To realize high selectivity for differential mode, another two TZs are created by the source-load coupling and coupling sections. Furthermore, wideband common-mode (CM) suppression is achieved. The fabricated filter has 3-dB fractional bandwidth ranging from 20.0% to 26.0% centered at 1.71 GHz and wideband suppression (17 dB from 2 to 4.4 GHz) for the differential mode, as well as common-mode suppression better than 20 dB from 0 to 4.5 GHz.

1. INTRODUCTION

Recently, BPFs with reconfigurable bandwidth have attracted attention as a means to meet the demand of the reconfigurable communication system. PIN diodes have been used for the conventional reconfigurable BPF with the discrete bandwidth [1–3]. By using eight PIN diodes, Rauscher proposed a reconfigurable BPF with two bandwidths of 500 and 1500 MHz centered at 10 GHz [1]. By employing a PIN diode to switch the number of transmission poles, Tu presented a reconfigurable BPF with the switchable fractional bandwidth (FBW) from 29% to 50% centered at 1.5 GHz [2]. Introducing PIN diodes in the liquid crystal polymer (LCP) based circuit, Miller et al. designed a reconfigurable coupled line BPF with the FBW ranging from 26% to 50% [3]. A filter with reconfigurable bandwidth (from 16.5% to 76.5%, centered at 0.42 GHz) were realized in [4] by using dual-behavior resonators and PIN diodes. On the other side, to achieve the continuously reconfigurable bandwidth of BPF, the varactor diodes are also utilized to tune the bandwidth. By introducing the variable coupling reducers, Sanchez-Renedo et al. proposed a varactor-tuned combline BPF with the tunable FBW from 0.4% to 2.1% [5]. By introducing surface acoustic wave resonators and BaSrTiO₃ (BST) varactor diodes, Kimura et al. proposed bandwidth-tunable filter [6]. However, none of above-mentioned reported works presents the separate low/high-side passband edge reconfigurability. Therefore, by employing a dual-mode triangular patch [7], triple-mode H-type resonator [8], a quadruple-mode resonator [9], and a stub-based resonator [10], tunable BPFs with the separate low/high-side edge reconfigurability of the passband have been reported.

Balanced BPFs play important roles in RF and microwave circuits with the advantage of higher immunity to the environmental noise. Two kinds of frequency-tuned balanced filter with constant absolute bandwidth (ABW) and FBW were reported in [11, 12] respectively. However, the BPFs with the fixed center frequency and tunable bandwidth play an important role in the many electronic measuring instruments (e.g., spectrum analyzer, network analyzer and advanced receiver). To the best of our knowledge, there has been little effort in developing the balanced BPFs with reconfigurable bandwidth.

Received 28 May 2015, Accepted 31 July 2015, Scheduled 23 August 2015

* Corresponding author: Wenjie Feng (fengwenjie1985@163.com).

¹ Department of Communication Engineering, Nanjing University of Science & Technology, Nanjing 210094, China. ² Faculty of Mathematics and Physics, Huaiyin Institute of Technology, 1 Meisheng Eastern Road, Huai-An 223001, Jiangsu Province, China. ³ School of Electronics and Information, Nantong University, 9 Seyuan Road, Nan Tong, Jiangsu Province 226019, China.

Thus, study of balanced filters with reconfigurable bandwidth becomes an important topic and very desirable in reconfigurable communication systems.

The motivation of this letter is to design a balanced BPF with tunable bandwidth based on a triple-mode stub-loaded resonator. The proposed resonator can generate one odd-mode and two even-mode frequencies inside the desire passband together with two TZs out of the passband. By properly controlling the stub's loading capacitances, the two even-mode frequencies and the two TZs can be tuned independently while the odd-mode frequency keeps constant. As a result, the separate low/high-side passband edge reconfigurability can be easily realized with the center frequency unchanged. Furthermore, another two TZs are created by the source-load coupling and coupling sections, resulting in high selectivity. Besides, desire differential-mode (DM) frequency response and wideband CM suppression are attained by a suitable choice of the balanced coupling sections.

2. PROPOSED TUNABLE BALANCED BPF

The configuration of the proposed balanced BPF is shown in Fig. 1. From port 1 to port 2 (port 1' to port 2') in Fig. 1, a symmetrical stub-loaded resonator is located in the centre of the balanced BPF and the balanced coupling sections are located at the both sides. Four microstrip lines ($Z = 50 \Omega$) are connected to ports 1, 1' and ports 2, 2'. C_{v1} , C_{v2} are the capacitances of the varactors (JDV2S71E and ISV232 from Toshiba) controlled by the biases of V_1 , V_2 ; C_1 , C_2 are the capacitances of the dc blocking capacitors. Four resistors ($51 \text{ k}\Omega$) are used as RF chokes to reduce the RF-signal leakage through the bias network. Furthermore, the source-load coupling is introduced to improve the selectivity.

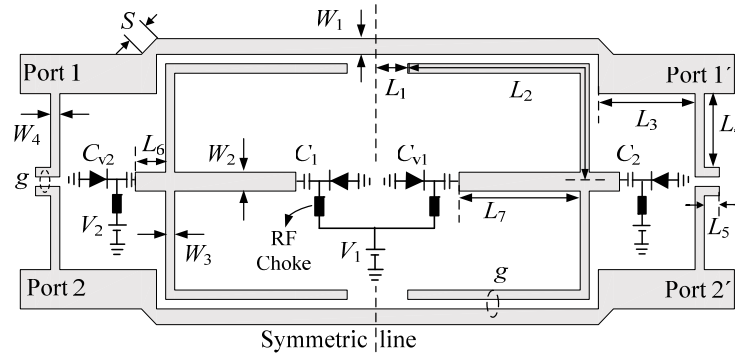


Figure 1. Configuration of proposed balanced filter.

2.1. Analysis of Resonant Frequencies and TZs

The basic element of the proposed balanced BPF is a triple-mode resonator, as shown in Fig. 2(a). It consists of a half-wavelength resonator and two open stubs loaded with variable capacitors on its central plane. Y_0 , $2Y_0$, l_1 , l_2 , and l_3 are the admittances and lengths for the transmission line sections C_{r1} , C_{r2} are variable loading capacitances of the stub. Since the resonator is symmetrical to the central plane ($T-T'$), the odd/ even-mode method is implemented. By placing a shorted/ open circuit at the symmetric plane ($T-T'$), the circuit model for odd and even circuits can be obtained, as shown in Figs. 2(b) and (c). The odd/even-mode input admittance Y_{ino} and Y_{ine} can be expressed by

$$Y_{ino} = \frac{Y_0}{j \tan \theta_1} \quad (1)$$

$$Y_{ine} = Y_0 \frac{Y' + jY_0 \tan \theta_1}{Y_0 + jY' \tan \theta_1} \quad (2)$$

$$Y' = jY_0 \left(\frac{0.5\omega C_{v1} + Y_0 \tan \theta_3}{Y_0 - 0.5j\omega C_{v1} \tan \theta_3} + \frac{0.5\omega C_{v2} + Y_0 \tan \theta_2}{Y_0 - 0.5j\omega C_{v2} \tan \theta_2} \right) \quad (3)$$

where $\theta_i = \beta l_i$, and β is the propagation constant of the transmission line.

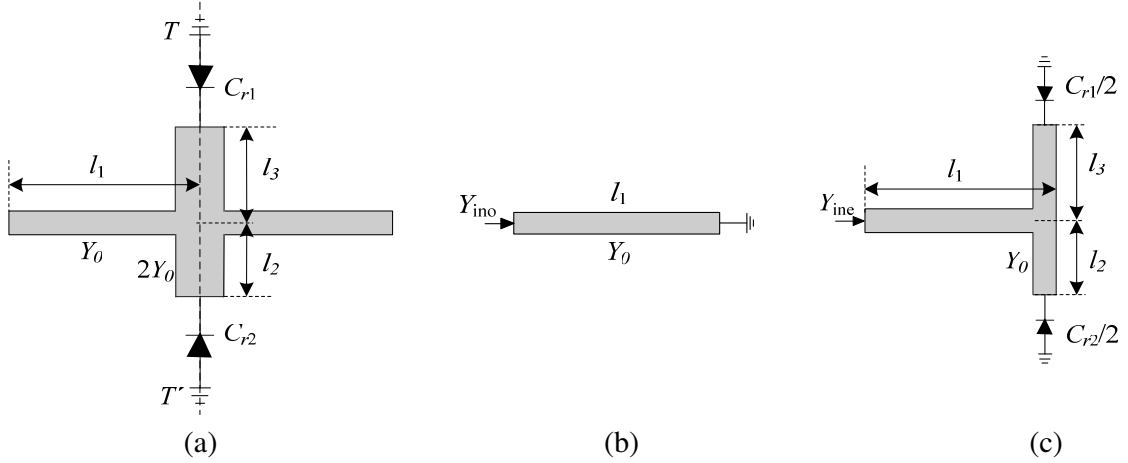


Figure 2. (a) Structure of proposed resonator, (b) odd-mode equivalent circuit, (c) even-mode equivalent circuits.

From the resonance condition of $\text{Im}(Y_{ino}) = 0$, the odd-mode resonance frequency (f_o) can be given as

$$f_o = \frac{(2n + 1)c}{4l_1\sqrt{\varepsilon_e}} \quad (4)$$

where $n = 1, 2, 3, \dots$ ($n = 0$ corresponding to fundamental resonance condition), c is the velocity of light speed in free space, and ε_e is the effective permittivity. From (4), it is concluded that the odd-mode resonance frequency doesn't depend on the loading capacitances C_{r1} and C_{r2} .

For the even-mode resonance condition, it can be seen from (2) and (3) that the even-mode resonance frequencies depend on the loading capacitances C_{r1} and C_{r2} . This characteristic of the proposed resonator can be used to design a BPF with tunable bandwidth and fixed centre frequency.

As analyzed in [13], one TZ can be introduced when the stub (l_2) loaded with the variable capacitor (C_{r2}) is under the resonance condition. TZ1 (f_{TZ1}) can be illustrated by

$$f_{TZ1} = \frac{1}{2\pi Z_0 C_{r2} \tan(\beta l_2)} \quad (5)$$

In the same way, another TZ can also be introduced when transmission line (l_3) loaded with the variable capacitor (C_{r1}) is under the resonance condition. TZ2 (f_{TZ2}) can be determined as follows:

$$f_{TZ2} = \frac{1}{2\pi Z_0 C_{r1} \tan(\beta l_3)} \quad (6)$$

It can be concluded from (5) and (6) that the TZ1 and TZ2 can be tuned by the capacitances C_{r2} and C_{r1} respectively. This property of the proposed resonator can be used to design a BPF with high selectivity.

In order to verify the theoretical analysis, the simulation was carried out using Advanced Design System (ADS) 2008. Two microstrip lines with characteristic impedance of 50Ω were utilized to feed the proposed resonator using loose coupling to investigate its resonance behavior. The other parameters in Fig. 3 are as follows: $\varepsilon_r = 2.2$, $h = 0.8$ mm, $l_1 = 40$ mm, $l_2 = 8$ mm, $l_3 = 25.8$ mm, $C = 0.03$ pF. When C_{r2} is fixed and C_{r1} varies from 0.2 to 0.3 pF (Fig. 3(a)), the higher even-mode resonance frequency (f_{e2}) and TZ₂ move towards lower frequency while the lower even-mode resonance frequency (f_{e1}), odd-mode resonance frequency (f_o) and TZ₁ are little affected. When C_{r1} is fixed and C_{r2} varies from 30 to 20 pF, f_{e1} and TZ₁ move towards higher frequencies while f_o , f_{e2} and TZ₂ keep almost unchanged. This characteristic of the proposed resonator can be used to design a BPF with tunable separate low/high-side passband edge, fixed centre frequency and high selectivity.

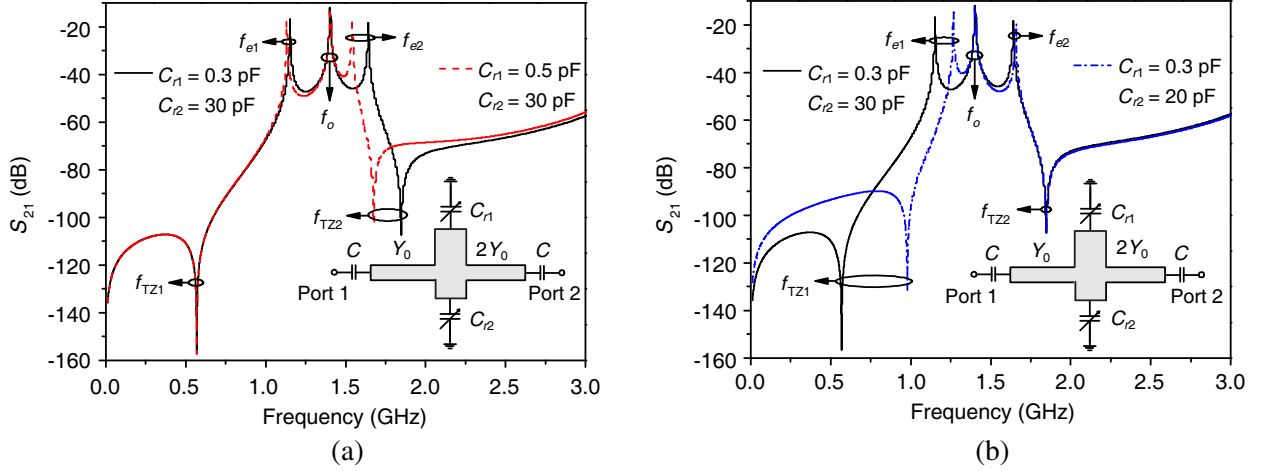


Figure 3. Resonance frequencies and inherent TZs against (a) C_{r1} and (b) C_{r2} .

2.2. Differential/Common-Mode Response

When the differential/common-mode signal is excited from ports 1 and 1' (shown in Fig. 1), the virtual shorted/open condition can be achieved along the symmetric line. The circuit structure of the proposed balanced BPF is shown in Fig. 4(a), and the corresponding differential/common-mode equivalent half circuit is shown in Fig. 4(b). Z_{oo} , Z_e and θ_1 are the odd/even-mode characteristic impedance and electrical length of the coupling sections. When the length of the coupling sections are about quarter wavelength at the centre frequency (f_{dd0}) of the DM passband, i.e., $\theta_1 \approx 90^\circ$, bandpass (for the differential mode) and all-stop (for the common mode) responses can be achieved [14]. In addition, the cross-coupled capacitance C_{cross} in Fig. 4(b) is realized by the capacitive coupling between the sections (Z_2 , θ_2) in Fig. 4(a), which is also the source-load coupling in Fig. 1.

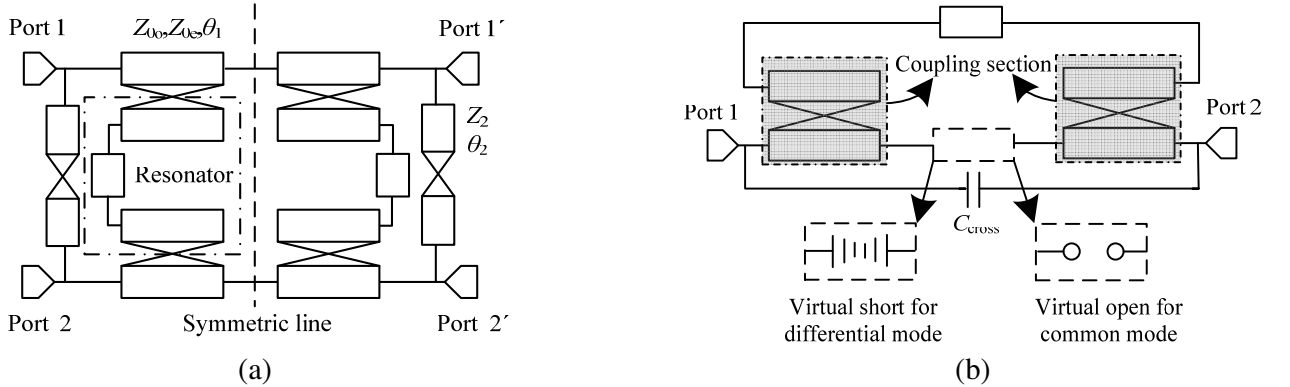


Figure 4. (a) Circuit structure, (b) differential/common-mode equivalent half-circuit.

In order to verify the theoretical analysis, the simulation was carried out using Advanced Design System (ADS) and High Frequency Structure Simulator (HFSS) on the substrate with $\epsilon_r = 2.2$ and $h = 0.8$ mm. The parameters in Fig. 1 are as follows: $W_1 = 3.4$ mm, $W_2 = 1.2$ mm, $W_3 = 0.2$ mm, $W_4 = 2.5$ mm, $L_1 = 4.2$ mm, $L_2 = 24.4$ mm, $L_3 = 5.3$ mm, $L_4 = 5.3$ mm, $L_5 = 1.0$ mm, $L_6 = 2.0$ mm, $L_7 = 21.2$ mm, $L_8 = 7.2$ mm, $S = 4.8$ mm, $g = 0.12$ mm, $C_1 = 0.5$ pF, $C_2 = 33$ pF, $V_1 = 19$ V and $V_2 = 7$ V. The simulated frequency responses of the proposed balanced BPF are shown in Fig. 5. There are four TZs which improve the DM selectivity. TZ₁ and TZ₃ are introduced by the shunt open stubs loaded with varactors, as analyzed above. TZ₂ is introduced by the source-load coupling scheme, while TZ₄ is realized when θ_1 is about 180° at $2f_{dd0}$. Furthermore, with the increase of k , the passband and

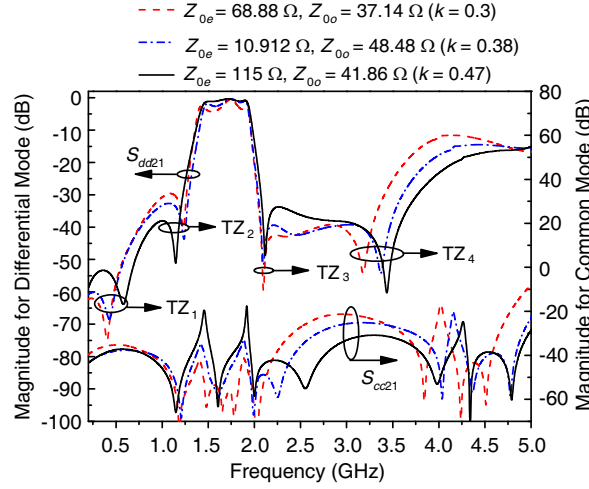


Figure 5. Simulated S_{dd21} , S_{cc21} against Z_{0o} , Z_e ($V_1 = 19$ V, $V_2 = 7$ V).

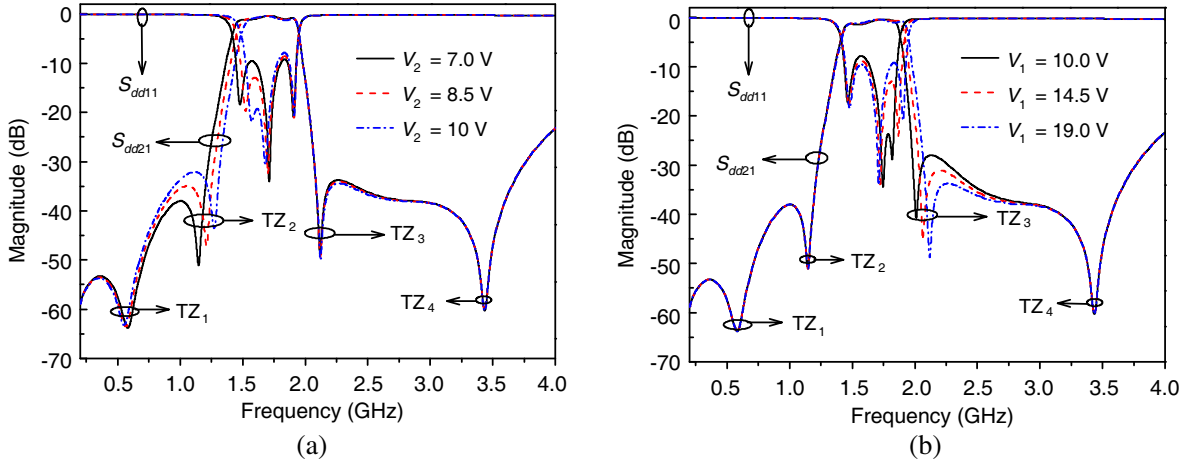


Figure 6. Simulated S -parameters of studied filter, (a) S_{dd21} and S_{dd11} against V_2 ($V_1 = 19$ V) (b) S_{dd21} and S_{dd11} against V_1 ($V_2 = 7$ V).

stopband performances for the DM signal are improved though the CM suppression in the DM passband is degraded. Here, $k(k = (Z_{0e}Z_{0o})/(Z_{0e} + Z_{0o}))$ means the coupling coefficient of the coupling sections, and Z_{0e} , Z_{0o} are the odd/even-mode characteristic impedance. Thus, suitable structure parameters of the coupling sections should be chosen to improve the DM responses while wideband CM suppression can be realized.

The simulated frequency responses of the proposed balanced filter for the differential mode against the reversed bias voltages V_2 and V_1 (shown in Fig. 1) are shown in Figs. 6(a) and (b). As shown in Fig. 6(a), when V_1 is fixed at 19 V and V_2 varies from 7 to 10 V, the higher even-mode frequency, odd-mode frequency, TZ_1 , TZ_3 and TZ_4 remain stationary while TZ_2 and the lower even-mode frequency move towards higher frequency. It can be seen from Fig. 6(b) that the higher even-mode frequency and TZ_3 move towards lower frequency, whereas the lower even-mode frequency, odd-mode frequency, TZ_1 , TZ_2 and TZ_4 remain the same when V_2 is fixed at 7 V and V_1 varies from 19.0 to 7.0 V. Thus, the low/high-side edge of the passband including the zeros near the passband edges can be tuned independently by the reversed bias voltages V_1 and V_2 .

Based on the above discussions, the proposed triple-mode resonator and balanced coupling structure with the source-load coupling can be explored for designing the high selectivity balanced BPF with tunable bandwidth while the wideband CM suppression can be also realized.

3. RESULTS AND DISCUSSION

Figures 7(a) and (b) show the results of the proposed tunable balanced BPF. Measurement was carried out using Agilent's N5230C network analyzer. The measured results show that the 3 dB bandwidth for the differential mode ranges from 340 to 445 MHz (20% ~ 26%) centered at 1.71 GHz (f_{dd0}) with better than 11.5 dB in-band return loss and less than 1.65 dB insertion loss. Furthermore, there are four TZs out of the passband, resulting in sharp cut-off response at both lower and upper stopbands with a good suppression of better than 17 dB from 2 to 4.4 GHz. In addition, over 20-dB common-mode suppression is obtained from 0 to 4.5 GHz ($2.63f_{dd0}$). Deviations between the simulated and measured results may be attributed to the bias circuit and fabrication accuracy. In terms of measured results, within the passband (1.49–1.93 GHz) the group delay is less than 3.5 ns, as shown in Fig. 8(a). The input third-order intermodulation intercept point (IIP3) is measured at $V_1 = 17$ V, $V_2 = 10$ V with 1-MHz frequency spacing. The IIP3 is measured about 34 dBm. Fig. 8(b) shows the photograph of the proposed BPF.

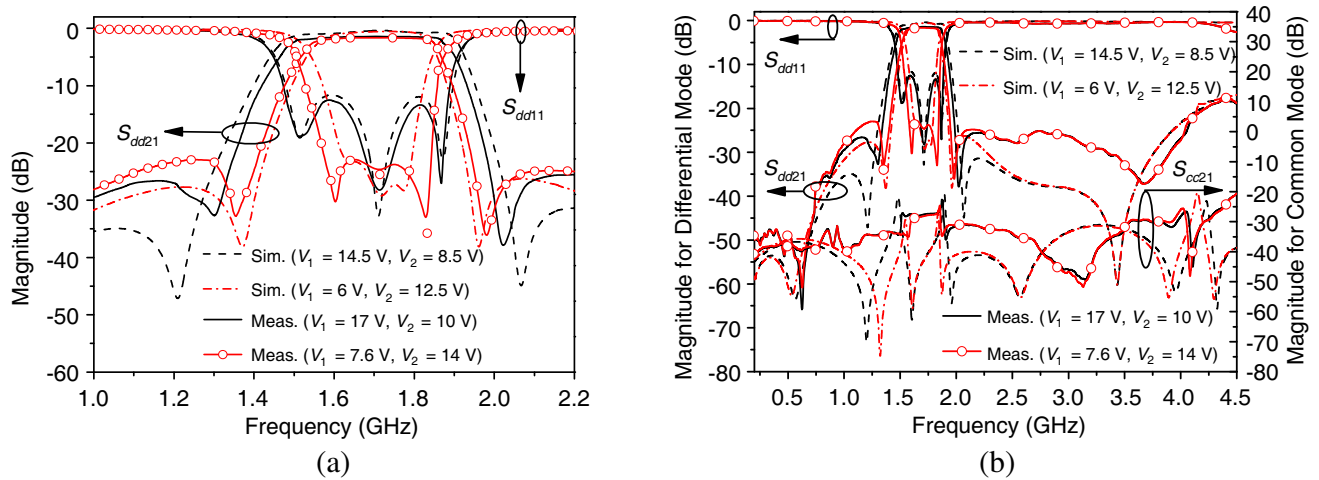


Figure 7. Results of proposed tunable balanced BPF, (a) narrowband responses, (b) wideband responses.

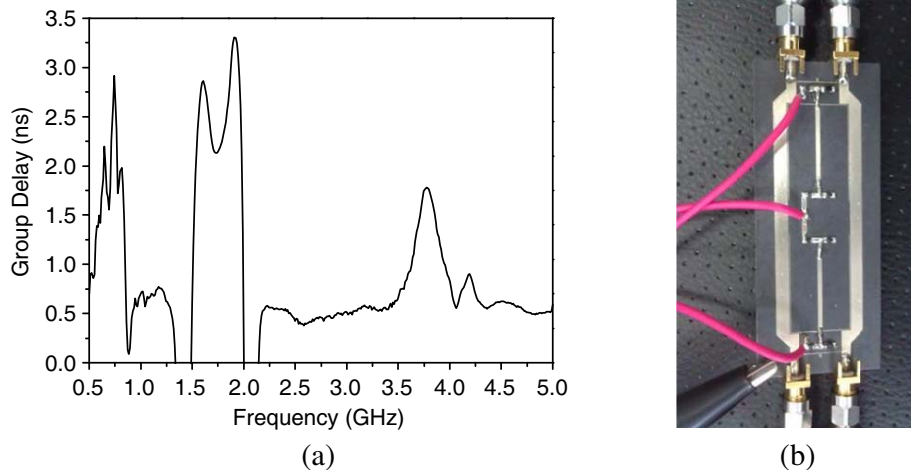


Figure 8. (a) Group delay and (b) photograph of proposed tunable balanced BPF.

4. CONCLUSION

This letter has proposed a tunable balanced triple-mode BPF. The tunable bandwidth and better common-mode suppression can be achieved with the proposed varactor-tuned resonator and suitable parameters of the coupling structure. Four TZs out of the DM passband are realized to improve the selectivity. The proposed BPF has the properties of tunable bandwidth, high selectivity, and wideband common-mode suppression. With all these good performance, the proposed new filter has potential application in communication systems.

ACKNOWLEDGMENT

This work is supported by the 2012 Distinguished Young Scientist awarded by the National Natural Science Foundation Committee of China (61225001), and by National Natural Science Foundation of China (6140010914), Natural Science Foundation of Jiangsu Province (BK20140791) and the 2014 Zijin Intelligent Program of Nanjing University of Science and Technology.

REFERENCES

1. Rauscher, C., "Reconfigurable bandpass filter with a three-to-one switchable passband width," *IEEE Trans. Microw. Theory Tech.*, Vol. 51, 573–577, 2003.
2. Tu, W.-H., "Compact low-loss reconfigurable bandpass filter with switchable bandwidth," *IEEE Microw. Wireless Compon. Lett.*, Vol. 20, 208–210, 2010.
3. Miller, A. and J.-S. Hong, "Cascaded coupled line filter with reconfigurable bandwidths using LCP multilayer circuit technology," *IEEE Trans. Microw. Theory Tech.*, Vol. 60, 1577–1586, 2012.
4. Lu, X., K. Mouthaan, and T. S. Yeo, "A filter with reconfigurable band edges using dual-behavior resonators," *Eur. Microw. Conf.*, Vol. 44, 1592–1595, 2014.
5. Sanchez-Renedo, M., R. Gomez-Garcia, J. I. Alonso, and C. Briso-Rodriguez, "Tunable combline filter with continuous control of center frequency and bandwidth," *IEEE Trans. Microw. Theory Tech.*, Vol. 53, 191–199, 2005.
6. Kimura, T., H. Kobayashi, and Y. Kishimoto, "Bandwidth-tunable filter consisting of SAW resonators and BaSrTiO₃ varactors directly fabricated on a LiTaO₃ wafer," *IEEE International Ultrasonics Symposium*, 795–798, 2014.
7. Serrano, A. L. C., F. S. Correria, T. P. Vuong, and P. Ferrari, "Synthesis methodology applied to a tunable patch filter with independent frequency and bandwidth control," *IEEE Trans. Microw. Theory Tech.*, Vol. 60, 484–493, 2012.
8. Chao, S.-F., W.-C. Lin, and C.-Y. Kuo, "Bandpass filter with tunable bandwidth using triple-mode H-type resonator," *International Symposium on Next-Generation Electronics*, 1–3, 2014.
9. Huang, X.-G., Q.-Y. Feng, and Q.-Y. Xiang, "Bandpass filter with tunable bandwidth using quadruple-mode stub-loaded resonator," *IEEE Microw. Wireless Compon. Lett.*, Vol. 22, 176–178, 2012.
10. Mao, J.-R., W.-W. Choi, K.-W. Tam, W.-Q. Che, and Q. Xue, "Tunable bandpass filter design based on external quality factor tuning and multiple mode resonators for wideband applications," *IEEE Trans. Microw. Theory Tech.*, Vol. 61, 2574–2584, 2013.
11. Li, Y. C. and Q. Xue, "Tunable balanced bandpass filter with constant bandwidth and high common-mode suppression," *IEEE Trans. Microw. Theory Tech.*, Vol. 59, 2452–2460, 2011.
12. Mao, J.-R., W.-Q. Che, Y.-L. Ma, and J.-X. Chen, "Tunable differential-mode bandpass filters with wide tuning range and high common-mode suppression," *IET Microw. Antennas Propag.*, Vol. 8, 437–444, 2014.
13. Chun, Y.-H. and J.-S. Hong, "Electronically reconfigurable dual-mode microstrip open-loop resonator filter," *IEEE Microw. Wireless Compon. Lett.*, Vol. 7, 449–451, 2008.
14. Pozar, D. M., *Microwave Engineering*, Wiley, New York, 1998.